Diffuse interstellar bands carriers and cometary organic material

Jean-Loup Bertaux, Rosine Lallement

Monthly Notices
of the
ROYAL ASTRONOMICAL SOCIETY

MNRAS **469,** S646–S660 (2017)
Advance Access publication 2017 August 31

doi:10.1093/mnras/stx2231

Diffuse interstellar bands carriers and cometary organic material*

Jean-Loup Bertaux[1]† and Rosine Lallement[2]†

[1]*LATMOS, Université de Versailles Saint-Quentin, 11 Boulevard d'Alembert, F-78280 Guyancourt, France*
[2]*GEPI, Observatoire de Paris, 6 Place Jules Janssen, F-92195 Meudon, France*

Accepted 2017 August 25. Received 2017 August 25; in original form 2017 March 21

ABSTRACT

We suggest that the large organic molecules found in the dust of comet 67P/CG originated from the interstellar medium (ISM), and that this material is the source of absorption features in stellar spectra known as diffuse interstellar bands (DIBs). These large organic molecules were present in the ISM prior to the emergence of the pre-solar nebula and were conserved during comet formation in the solar nebula due to gentle, hierarchical accretion, a scenario based on many lines of evidences collected with *Rosetta rendezvous* mission (Davidsson et al. 2016). This is in contrast with the sublimation of H_2O ice, according to diverse comet D/H values. While the organic to mineral mass ratios R_C for comet Halley and 67P/CG were measured in the range ∼0.32–1.0, we estimate that the DIB carriers alone can provide $R_{ISM} = 0.32$, but that this ratio could be increased by other organic molecules in the ISM that do not show up in absorption. The decrease of DIB during line-of-sight crossings of the dense cores of interstellar clouds and the simultaneous steepening of the far-UV part of the reddening curve suggest that DIB carriers coagulate and are constituent of the very small grains eventually preserved in comets. This conclusion implies that a future sample-return mission of a comet nucleus would not only provide unique information on comets, but also on the exact nature of the interstellar species producing the hundreds of DIBs, an unanswered question since their discovery several decades ago.

Key words: comets: general – comets: individual: 67P/Churyumov – Gerasimenko – protoplanetary discs – dust, extinction – ISM: lines and bands – ISM: molecules.

1 INTRODUCTION

Comets are thought to be the most primitive bodies of the Solar system, remnants of the formation process in which a cloud of interstellar (IS) material collapsed under the effect of self-gravitation. The central part of pre-solar nebula (PSN) became the Sun, while several planets formed from the material spread in a disc, together with comets at distances 15–30 au from the Sun. The ESA *Rosetta* space mission to comet Churyumov–Gerasimenko (67P/CG) ended in 2016 September with the *Rosetta* orbiter impacting the surface of the nucleus, concluding over 2 yr of observations, including those from the *Philae* lander and providing an unprecedented wealth of data on the activity, composition and structure of a comet nucleus, allowing the inference of scenarios related to the formation and evolution of comets in general.

Since the initiation of the *Rosetta* project in the 1980s, many advances have been made in the field of physics and chemistry of the interstellar medium (ISM), the very material from which condensed the Solar system. One technique characterizes the ISM material by studying the absorption imprinted on the spectrum of a star. In particular, diffuse interstellar bands (DIBs) are absorption features recorded in the spectra of stars in the visible and near infrared. The most likely source of these features are organic molecules (DIB carriers) in the gaseous phase of the ISM, which can be traced to the other components of the ISM: H, H_2 and IS dust reddening the stellar spectra. They probably constitute '... the largest reservoir of organic matter in the Universe' (Snow 2014). Since the primitive solar nebula formed from a cloud of ISM material, these DIB carriers were certainly present in the early stages of the formation of the Solar system. Such material would have survived the radiation of the early Sun if located in the outer regions of the Solar system, beyond the orbit of Neptune at 15–30 au, in the same location comet nuclei formed and survived, creating the present Edgeworth–Kuiper belt. The subsequent survival of these molecules during this cometary nuclei formation period is then necessary to explain the direct connection with DIB carriers in the ISM. We suggest that before the initial steps of accretion a number of these complex molecules coagulated onto very small grains (VSGs) or themselves formed VSGs, which were subsequently coated with ice in molecular cores, in agreement with

*MNRAS special edition called 'Comets: A new vision after *Rosetta* and *Philae*'.

† E-mail: jean-loup.bertaux@latmos.ipsl.fr (JL-B); rosine.lallement@obspm.fr (RL)

some recent IS dust models (Jones 2016). During the subsequent gentle accretion process of comet nuclei formation (Davidsson et al. 2016), they survived the evaporation of the icy mantles and the small grain agglomeration to finally constitute a large fraction of the refractory organic material massively present in the solid part of cometary nuclei. In this case, a significant number of DIB carriers would correspond to the so far unidentified large organic molecules (LOMs) whose existence is deduced from the COSIMA experiment (Fray et al. 2016).

The gaseous coma of comets contains an abundance of carbon-based molecules, the first sign of organics in comets. This was established prior to the identification of H_2O indirectly from H Lyman α emission (Bertaux & Blamont 1970) and then directly from its infrared emission. The visible spectrum of gas coma emission is dominated by spectral lines revealing carbonated small molecules (C_2 and its Swan spectroscopic system, C_3, CN, CH and CH^+; Cochran & Cochran 2002). They are certainly photodissociation daughter products of organic mother molecules escaping the nucleus.

Radio observations of the huge comet C/1995 O1 (Hale–Bopp) in the millimetre and submillimetre bands enabled the discovery of four new organic molecules (defined here as having at least one carbon atom and one H atom), new members of the family of cometary molecules listed in table 4 of Bockelée-Morvan et al. (2000). This list contains 14 organic molecules, with 1 or 2 C atoms at most, and 11 of them are also identified in particular regions of the ISM, so-called hot cores and the bi-polar flow of radio object L1157. We note however that in the ISM, radio observations have identified a large number of organic molecules, but all of them with a number of carbon atoms $N_C \leq 11$. In this paper, we focus our attention on larger organic molecules, with little discussion of the small organic molecules (SOMs).

The first detection of organic matter in cometary dust was made during the encounter of Vega 1, Vega 2 and Giotto space probes with comet Halley in 1986. The PIA/Giotto and PUMA/Vega time-of-flight (TOF) mass spectrometers analysed individual dust particles vaporized upon impact within the detectors, and so-called CHON particles were denominated due to their high content of C, H, O and N atoms, present together with a mineral phase (Kissel, Sagdeev & Bertaux 1986; Sagdeev et al. 1986; Langevin et al. 1987). On Vega 2, spectral features of the UV emission (342–375 nm) were assigned to the fluorescence of phenantrene by comparison with a laboratory spectrum (Moreels et al. 1994). This $C_{14}H_{10}$ molecule followed a parent molecule radial profile in the coma. It is a typical polycyclic aromatic hydrogenated (PaH) molecule, containing three hexagonal (benzenic) carbon cycles. Another Vega 2 observation of emissions around 376 nm was also tentatively assigned to pyrene, a four-cycle PaH (Clairemidi et al. 2004). The phenantrene molecule and other forms of PaHs have been considered to be responsible for IR emissions at 3.28 μm in some nebulae, assigned to X–CH organic compound vibrational transition (Léger & Puget 1984) and also for some of the DIB absorption bands. Both phenantrene and pyrene are constituents of the organic material found in the carbonaceous chondrites of Murchison meteorite (Pering & Ponnemperuma 1971). Following our hypothesis, it is possible that organic molecules detected in fluorescence in P/Halley coma could have been produced by fragmentation of DIB carriers when dust particles sublimated from the nucleus surface or in flight in the coma.

A direct signature of DIB carriers in comets has previously been investigated. Several emission features near 443 nm detected in the inner coma (<780 km) of the bright comet Hyakutake (C/1996 B2), passing near the Earth in 1996, were tentatively related to the 443 nm DIB absorption feature (A'Hearn et al. 2014). Follow-up observations with high spectral resolution of this DIB in absorption on target stars did not show the same detailed structure as the cometary emission did (Snow 2002), casting some doubt on the assignment to the same DIB carrier molecule. However, a solar fluorescence emission spectrum of a given molecule might not be identical to its absorption spectrum, and so the relationship between the 443 nm comet emission and the 443 nm DIB absorption feature is probably still open.

In the next section, we describe some recent results of *Rosetta* relevant to our hypothesis. The significance of the various (D/H) in H_2O for different comets is then discussed in Section 3, calling for an episode of sublimation of IS ices during the formation of the Solar system, and before the formation of comets. We argue that this scenario is not in contradiction with our claim of unprocessed organic material from the IS cloud to comets. Section 4 describes our current knowledge of DIBs, some aspects of the physics of the DIB carriers, and a quantitative estimate of the fraction of ISM carbon locked into the DIB carriers. In Section 5, we compare the organics to minerals mass ratios in the ISM and in the comet. They are found to be similar within a factor of 2, compatible with our hypothesis of direct integration of ISM DIB carrier molecules into the nucleus of a comet. The final section concludes advocating a non-cooled comet sample return mission as a way to investigate the DIB carriers in the laboratory.

2 SOME RESULTS FROM *ROSETTA*/*PHILAE* INVESTIGATIONS ON COMET 67P

2.1 Formation of comets

The degree of processing of IS material in the primitive solar nebula has been the subject of many discussions, ranging from zero processing (at least in the outer parts of the solar nebula where comets were formed) to full destruction of IS molecules and grains, and reformation of molecules, ices and solid grains. One major outcome of the *Rosetta* mission's investigation of the nucleus of comet 67P Churyumov–Gerasimenko is the idea that this comet is not a reassembly of the debris of large (∼200 km) trans-Neptunian objects (TNO) after collisions, but the result of a gentle, hierarchical process, growing slowly from IS material up to the size of the nucleus (or one of the two lobes which constitutes the nucleus of 67P/CG) at very small relative velocities (Davidsson et al. 2016). This conclusion is based on a number of arguments, including the presence in the coma of supervolatile gases (CO, Ar, N_2, O_2, CO_2; Bieler et al. 2015; Hässig et al. 2015; Rubin et al. 2015) calling for permanent low temperatures, which precludes an evolutionary path via large TNO bodies that experience radio-active heating. Within this formation scenario of the nucleus, it is quite logical to imagine that the DIB carriers present in the outskirts of the primordial solar nebula (15–30 au) were not chemically affected, but aggregated gently to become part of the organic material that is found now in the nucleus of 67P.

2.2 Small organic molecules in dust and the gaseous coma

Some solid material was collected during the first touchdown of *Philae* by chance, from the cloud of solid particles produced upon impact. Dust particles entered the COSAC mass spectrometer, and sublimation products of outgassing in the instrument were analysed in the 'sniffing mode' 25 min after collection while *Philae* was

flying at more than 100 m from the surface in its first bounce. The resulting *m*/*z* spectrum allowed inferring some molecules whose fragmentation pattern matched the observed spectrum. A number of molecules with one to three carbon atoms are inferred (Goesmann et al. 2015) in addition to HCN and CH_4. Several of these organic molecules have also been identified in the coma by the *Rosetta* mass-spectrometer ROSINA, as part of the famous 'zoo' (Altwegg 2016, ESA blog), such as methylamine (CH_3NH_2), acetonitrile (CH_3CN), acetaldehyde (CH_3CHO) and ethylamine ($C_2H_5NH_2$). It is likely that these COSAC inferred molecules were present in the solid material on the ground of the comet, which was composed of grains detached form the nucleus and redeposited there since the previous perihelion or before. They were not stored in water ice, at least since a few years. This COSAC finding suggests strongly that the gaseous species measured by ROSINA in the coma are coming from two different reservoirs in the comet: all the sublimating ices and everything that was trapped in them, and the non-icy refractory material. This is a fundamental new result of the mission. However, whether these molecules have spent their whole life trapped in the organic material, or in ices and then migrated recently to the refractory solid phase is still an open question. In this respect, we note some consistency between the comet situation and the ISM. Most of the simple organic molecules identified in the coma have been also found in the ISM in locations that are certainly full of LOMs at the origin of DIBs. It could be very well that their coexistence in the solid material of the comet and the ISM is not a pure coincidence. In both cases, all the observed molecules are separated and free floating, but prior to their evaporation these small molecules could be trapped in the coagulated bunch of LOMs, and trapped by Van der Waals forces. LOM detections at the 67P have only been reported in data from the COSIMA instrument by Fray et al. (2016) discussed in the next section.

2.3 Large organic molecules

Here, we distinguish LOMs as having six or more carbon atoms $N_c > 6$, allowing one or more benzenic hexagonal cycle and SOMs, as $N_c < 6$. In the ISM, a large number of molecules have been formally identified by their microwave signature but up to now all with less than 11 carbon atoms. As mentioned previously, a large number of these SOMs have also been found in the gaseous coma of comets. We will not discuss these SOMs any further other than to note that, if the cometary gaseous SOMs are preserved from their original ISM counterpart, a fortiori the larger organic molecules that are found in the solid phase (refractory organics) of comets could also have survived intact, as we suggest for the DIB carriers in this paper.

The IR reflectance of 67P/CG shows a broad absorption feature in the 2.9-to-3.6 μm interval 'compatible with opaque minerals associated with non-volatile organic macromolecular material' (Capaccioni et al. 2015), suggesting the presence of C–H and/or O–H chemical groups. Solid grains collected by the COSIMA experiment onboard *Rosetta* have been photographed and analysed individually with time-of-flight secondary ion mass spectrometry (TOF-SIMS) technique. The *m*/*z* spectra (Fray et al. 2016) are dominated by C^+, CH^+, $CH_2{}^+$ and $CH_3{}^+$, which the authors argue are fragments of much heavier molecules in the collected grains. These spectra show a striking similarity with those collected from the organic parts of Murchison and Orgueil meteorites. Indeed, Fray et al. (2016) note that their COSIMA analysed comet material '. . . could have the same origin [interstellar medium and/or the solar nebula] as the meteoritic insoluble organic matter, but suffered less modification before and/or after being incorporated into the comet'. Here, we go a step further and suggest that this very comet material is composed at least partially of DIB carriers, ubiquitous in the ISM.

Up to now, the only ISM DIB carrier that has been identified with great confidence (by comparison with laboratory measurements) is the ionized fullerene molecule $C^+{}_{60}$ (whose shape is like a soccer ball made of hexagons and pentagons), with two strong absorption bands at 9632.7 and 9577.5 Å, features first identified in diffuse IS clouds by Foing & Ehrenfreund (1994), confirmed later by laboratory measurements (Campbell et al. 2016). In parallel, it is remarkable that a mass spectrum of the complex organic phase material of Allende meteorite (Becker, Bunch & Allamandola 1999) shows the presence of fullerene C_{60}, (mass 720 amu). This suggests strongly that IS organic material (in particular, DIB carriers) might have been directly incorporated in the parent body of the meteorite, making the so-called insoluble organic material that constitutes up to 4 per cent of some meteorites. A fortiori the same thing could have happened in cometary nuclei, which suffered certainly less processing than meteoritic material.

3 IMPLICATIONS OF THE DIVERSITY OF D/H RATIO IN COMETARY WATER VAPOUR

The central idea of this paper is to suggest that IS organic material, notably the DIB carrier molecules aggregated in IS grains, were incorporated directly into comet nuclei without processing. In this section, we aim to show that this is not in contradiction with current models of the PSN, which are constrained by another powerful diagnostic: the D/H ratio found in comets (i.e. Bockelée-Morvan et al. 1998). Indeed, in a recent review of this subject, Ceccarelli et al. (2014) have presented the D/H ratio in the Solar system as 'Ariadne's thread' of the labyrinth of Solar system evolution from the collapse of a molecular cloud. Here, we concentrate only on comets.

3.1 The diversity of D/H measurements in comets

As reviewed by Bockelée-Morvan et al. (2015), there are now measurements of D/H ratios in water for a substantial number of comets (nine in Table 1). With 1/P Halley showing about twice more D/H than Earth oceans, along with a series of other comets measurements with high ratios, it was argued that comets could not have been the major provider of water on Earth through bombardment. However, measurements of 103P Hartley 2 (Hartogh et al. 2011) gave a D/H ratio similar to that of Earth, re-opening the discussion. *Rosetta* measurements by the ROSINA instrument showed C67P had a water D/H ratio ∼three times larger than Earth, concluding that comets could not have provided more than 10 per cent of Earth oceans (Altwegg et al. 2015). We propose that this diversity of cometary water ice indicated by the water D/H ratio [$(D/H)_{H2O}$ in the following discussion] suggests that IS water ice was not incorporated directly in cometary nucleus in the form of ice, but was rather a signature of different physical local conditions at the birth place of each comet, dictating the D/H ratio in water when it condensed into ice (and never changed since). This is developed further in the next section.

3.2 Interstellar ice sublimation and high accretion rate episode

The 'dirty snow ball' concept popularized by Whipple (1951) described the comet nucleus as a solid body, formed of a mixture of ices (mainly water) and dust in about equal mass proportions. In the

Table 1. (D/H) in water measured in comets and fractionation factor *f*.

Ref#	Object	(D/H) in water	*f* with respect to interstellar[a]
1	Earth (SMOW)	$(1.558 \pm 0.001) \times 10^{-4}$	6.9 ± 0.004
2	1/P Halley	$(3.1 \pm 0.34) \times 10^{-4}$	13.8 ± 1.5
3	C1996 B2 (Hyakutake)	$(2.9 \pm 1) \times 10^{-4}$	12.9 ± 4.4
4	C/1995 O1 Hale–Bopp	$(3.3 \pm 0.8) \times 10^{-4}$	14.7 ± 3.5
5	C2002 T7 (LINEAR)	$(2.5 \pm 0.7) \times 10^{-4}$	11.1 ± 3.1
6	8P/Tuttle	$(4.1 \pm 1.5) \times 10^{-4}$	18.2 ± 6.4
7	C/2009 P1 (Garradd)	$(2.06 \pm 0.22) \times 10^{-4}$	9.2 ± 1
8	C/2001 Q4 (NEAT)	$(4.6 \pm 1.4) \times 10^{-4}$	20.4 ± 6
9	103P/Hartley 2	$(1.61 \pm 0.24) \times 10^{-4}$	7.15 ± 1.1
10	67P Churyumov–Gerasimenko[b]	$(5.3 \pm 0.7) \times 10^{-4}$	23.5 ± 3.1

column 1: comet reference number for figure 2.
column 2: name of comet and Earth.
column 3: measured (D/H) ratio in comet H_2O.
column 4: D enrichment fractionation factor w.r.t. ISM.
[a]The IS D/H value has been taken here with the new value of 22.5 ppm (Weinberg 2016), 87 per cent of the big bang value of 25.8 ± 1.3 ppm. The often quoted value of 15 ppm is inappropriate (see Linsky et al. 2006), since it represents the particular region of the ISM in which we are presently embedded, which is poorer in observable gas phase D/H than further out, very likely because of preferential sticking of D atoms on IS grains (Draine 2003).
[b]All values of D/H are taken from Bockelée-Morvan et al. (2015), where appropriate references may be found, except for 67P Churyumov–Gerasimenko whose value is taken from Altwegg et al. (2015).

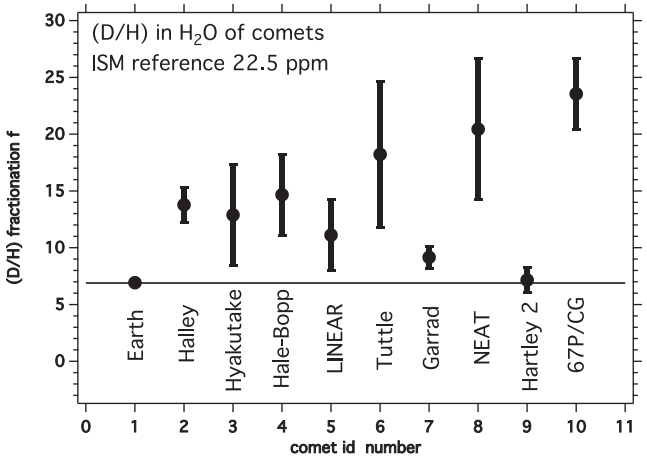

Figure 1. The measured water (D/H) fractionation factor in Earth oceans and in various comets with respect to the IS value as a function of reference number in column 1 of Table 1 (in approximate order of publication). The reference (D/H) ratio for the ISM is taken as 22.5 ppm (Weinberg 2016). A horizontal line is drawn at Earth's value.

frame of such a comet description, Greenberg (1982) popularized the idea that IS grains could have agglomerated into cometary nuclei during their formation. In the aftermath of Vega and Giotto space missions to comet Halley, Greenberg (1998) described his model of an individual IS grain, constituted by a silicate core embedded in three outer layers (mantles): the inner one constituted of a diffuse cloud organic refractory component, the second with a molecular cloud refractory component, and the outer mantle made of ices of H_2O and CO. In this scenario, the H_2O ice never sublimated from the IS stage through the PSN stage and was incorporated directly into the comet body. This scheme was inspired by observations of a few dense molecular clouds of ISM showing the presence of dust grains with an icy mantle of H_2O. In addition, it is commonly believed that, at the very low temperatures (∼10–20 K) encountered in dense molecular clouds, the water ice was very much enriched in HDO (a factor $f = 25$ versus the ISM bulk value is a commonly quoted value, Drouart et al. 1999).

Today, the variety of D/H ratios in comets contradicts the above idea that water ice found in comet nuclei is pre-solar, never sublimated and comes directly from the mantle of IS icy grains. Indeed, if the cometary H_2O ice came directly from the IS cloud which our protosolar nebula condensed from, we would expect a uniform D/H ratio in cometary water from comet to comet, characteristic of the primordial signature of H_2O ice in IS grains of our original molecular cloud. This hypothesis would be compatible with the observations of a roughly constant HDO/H_2O ratio around $f = 10$–15 (Fig. 1), from all comets before 103P Hartley 2. However, a wide range of values is observed, with 103P Hartley 2 comparable to Earths ($f = 7$) and 67P/CG up to three times the terrestrial value ($f = 23.5$).

This diversity implies that IS ice did sublimate early in the history of the nebula, and that $(D/H)_{H2O}$ was modified by some subsequent process or processes before the formation of comets, likely depending on the distance to the Sun. Indeed, thermal models of the collapse of the PSN have shown that during the rapid accretion phase to form the central star, gravitational energy is transformed into radiation, and the luminosity of the central regions may reach 30–50 times the final Sun luminosity. This central radiation heats the nebula to temperatures high enough for H_2O ice to sublimate completely up to a distance which depends on the luminosity: typically $T > 125$ K up to 15–30 au in the sophisticated accreting PSN model of Chick & Cassen (1997). This distance interval is thought to be where comet formed.

The Chick and Cassen model depends on various parameters, among which the opacity of dust, the efficiency of the accretion (which dictates the luminosity of the Sun and the inner part of the accretion disc) and the presence of a cavity around the Sun. Models with inefficient accretion (resulting in a luminosity only slightly larger than the Sun luminosity) predict that in the region 15–30 au, water would be in the form of ice (cavity or not). Only models with an efficient accretion, and therefore much larger luminosities (factor 30–50) produce temperatures $T > 125$ K (sublimation of ice), compatible with gaseous H_2O at 15–30 au. Therefore, based on current thermal models of the PSN, the diversity of (D/H) in comets implies the sublimation of IS ices provoked by a single episode of rapid accretion ($\sim 10^{-6}$ M_{sun} yr^{-1}).

3.3 Fractionation of deuterium in the solar nebula

Models predict that after internal disc accretion ended, luminosity dropped, temperature decreased throughout the nebula and the snow line (the line around 140–160 K separating the gaseous and recondensed ice crystal regions of H_2O) recessed rapidly to the centre (i.e. Kavelaars et al. 2011). How does entirely sublimated IS H_2O ice, uniformly and highly enriched in Deuterium evolve to produce the presently observed D/H diversity (Earth, meteorites, IDPs and then comets)? In order to explain this diversity, a processing mechanism of *f* decrease from a higher IS value is needed, a mechanism that likely includes a dependence on distance to the sun and/or temperature. We detail two proposed mechanisms in the following and discuss their consequences.

In the model of Kavelaars et al. (2011), similar to Drouart et al. (1999), a uniform fractionation *f* of the order of 25 is taken

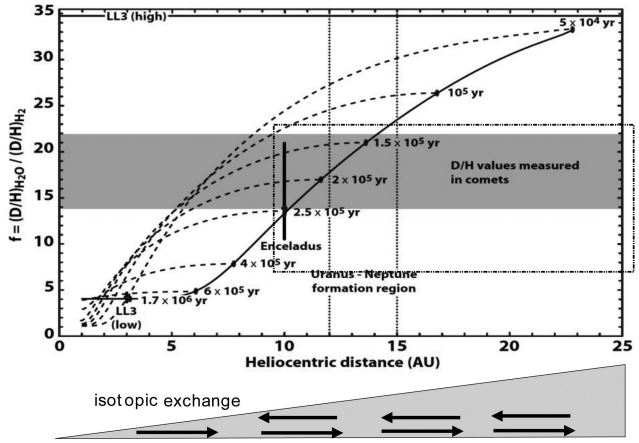

Figure 2. *Top*: the (D/H) fractionation ratio f (enrichment factor) in comets as a function of solar distance in the model of Kavelaars et al. (2011). The dashed curves trace the evolution of f in the gas phase before condensation and terminate by a dot at the point and time at which water vapour is frozen. The solid curve indicates the value of f reached at freezing time as a function of distance of the freezing point to the Sun after (fig. 1 from Kavelaars et al. 2011). The rectangular frame encompassing D/H in comets (dot–dashed line) has been extended to account for more recent observations. *Bottom*: schematic of the motion of the gas phase due to radial mixing in the model, necessary to impoverish water vapour (initially assumed at $f = 35$) by isotopic exchange with H_2 in the hot inner part (inspired from Ceccarelli et al. 2014).

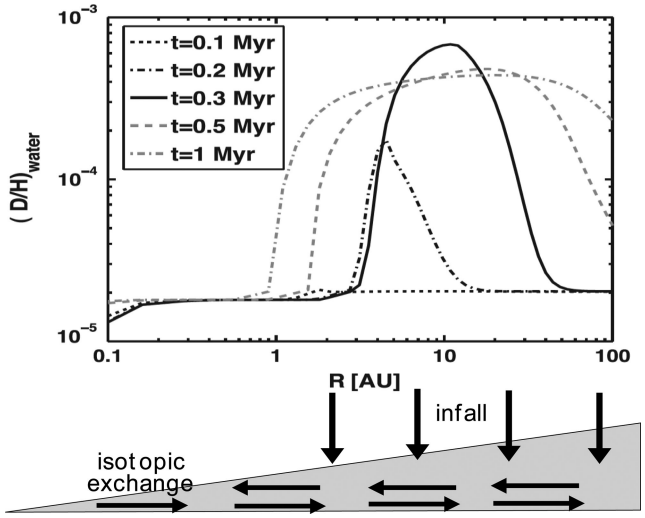

Figure 3. *Top*: the $(D/H)_{H2O}$ ratio in comets as a function of solar distance in the model of Yang et al. (2013). There is also radial mixing, but in addition chemical reactions are included which produce an indirect isotopic exchange with H_2, coming down to Earth value very fast (0.1 Myr). Adapted from Yang et al. (2013). *Bottom*: in this model some additional enrichment would come from infalling ice from the cloud onto the disk at various distances to explain the observed ratio in various comets.

as an initial condition for water vapour in the whole nebula, and the evolution of f is uniquely assigned to direct isotopic exchange with D-poor H_2. During a collision, two molecules of H_2 and H_2O may exchange their D atom, according to the following isotopic exchange reaction:

$$HDO + H_2 \leftrightarrow HD + H_2O. \quad (1)$$

The equilibrium fractionation factor $f = ([HDO]/[H_2O])/([H_2]/[HD])$ depends on the temperature T with an approximate law (Thi, Woitke & Kamp 2010):

$$f \approx 1 + 0.22 \times 10^6/T^2. \quad (2)$$

Typical equilibrium values are $f = 15$ at 125 K, 6.5 at 200 K and 3.44 at 300 K. However, the reaction rates of (1) (both direct and reverse) are very slow at low temperatures, and equilibrium with H_2 cannot be reached in a reasonable time-scale compatible with the history of the early Solar system (10^5–10^6 yr). Only in the central part near the Sun is the temperature sufficient to modify $(D/H)_{H2O}$ and bring it towards low values down to $f = 1$ or 2 in a reasonable time. However, with the addition of some amount of radial mixing of the material between the central part and outer regions, processed H_2O (abundantly poorer in D than $f = 25$) may be carried out to larger distances (Fig. 2), up to the freezing point where ice then keeps the local f factor. The distance of this freezing point depends on the thermal evolution of the nebula, and therefore depends on time and distance to the Sun. In this scenario, it is clear that comets poorer in D are frozen nearer the Sun than the comets richer in D, whose water vapour has been less processed. For instance, in the model of Kavelaars et al. (2011) (Fig. 2) the D/H increases monotonously with radial distance from $f = 4$ in the inner Solar system to $f = 32$ at 24 au.

As mentioned previously, before the observation of 103P/Hartley 2 and its low f value $= 7.15 \pm 1.1$ (∼terrestrial), other comets had been observed with $f \sim 12$–20, fitting nicely with the scenario above, at formation distances larger than 10 au, and with f values increasing with distance to the Sun. However, the Hartley 2 value is inconsistent and would require a formation distance <7 au from the Sun, too near the Sun to be acceptable.

The new model of Yang et al. (2013) included two additional novelties with respect to the model of Kavelaars et al. (2011). The first was the inclusion of chemical reactions with radicals like H, D, OH and OD. The end results of the extended network of chemical reactions is again a transfer of D atoms from water vapour to H_2, but in a much faster way at the same temperature as if only the direct isotopic exchange is considered. As a result, D-poor water processed near the Sun is 'pushed outwards due to the viscous spreading' and very quickly the factor f is ∼1 up to large distances, which cannot explain the observed f value of comets. In order to avoid this rapid and global decrease, Yang et al. (2013) introduced a second novelty: 'During the period of disk building, in-falling material from the molecular cloud [therefore, with D-rich H_2O] are added to and well mixed-vertically within the disk. . . ', as sketched in Fig. 3. In this scenario, comets with a low D/H ratio could be born further out than richer ones, in contradiction to the Kavelaars et al. (2011) model.

A simple alternate scenario could provide a more orderly profile of cometary birth locations, where $(D/H)_{H2O}$ increases with distance from Sun. Clearly, the neutral–neutral reactions with radicals H, D, OH, OD. . . must be included in models, since they do exist. But the effect of solar distance is fully dependent on the radial mixing parameters, because water vapour has to be brought in the warm inner part for more efficient chemical reactions. Therefore, it is certainly possible to reduce the radial mixing to such a point where the effect of neutral–neutral reaction with radicals will simply decrease with distance, diluting the originally D-rich H_2O, and replacing with the D-poor H_2O from the hot central solar region, without the need for any new infall. The thermal evolution is also important, since it dictates the time at which the (D/H) ratio is literally frozen in the comet material. Further modelling is needed in the future to address this. However, we retain the point that the

full sublimation of IS ice is not incompatible with the range of D/H measurements.

3.4 Summary on cometary (D/H)

In summary, the observed diversity of $(D/H)_{H2O}$ ratios in comets excludes the possibility that IS ice survived the formation of the Solar system up to its inclusion in comet nuclei. Sublimation of ice at least up to the distance of formation of comets, requires an episode of high central luminosity (30–50 L_{sun}) and a fast accretion rate of 10^{-5}–10^{-6} M_{sun} yr^{-1}. However, even in this model, the temperature stayed below ∼250 K in the region 10–30 au (Chick & Cassen 1997), leaving the organic IS material intact.

This diversity of comets requires a rather strong radial gradient of the $(D/H)_{H2O}$ at the time and location of re-freezing and formation of comets. This gradient may be explained by a mixture of local H_2O (D-rich) and H_2O (D-poor) reprocessed in the warm inner part of the nebula and transported outward (sketch of Figs 2 and 3). It was shown (Yang et al. 2013) that the indirect isotopic exchange through neutral–neutral reactions implying, O, H, D, H_2, HD, OH, OD... is much more efficient than the direct isotopic exchange reaction between H_2 and H_2O in the gas phase. The required radial gradient of $(D/H)_{H2O}$ may then be obtained by a moderate radial mixing (as we advocate above) or by the vertical infall of new IS material as suggested by Yang et al. (2013). In both cases, many IS grains would have kept their organic material, while water ice was likely sublimated, because a tiny icy grain *cannot* sublimate partially.

There is one possibility that cannot be excluded totally: the richest-D comets (possibly 67 P at $f = 23$) could have been agglomerated from IS icy grains that never sublimated and kept their IS $(D/H)_{ice}$ ratio. In this case, the organic material of the comet would a fortiori have preserved its IS composition, made of small grains, DIB carriers and similar organic molecules as we suggest in this paper.

Though it is out of the scope of this paper, we note that some other fractionation mechanisms, which play an important role in atmospheric physics, are still usually not included in PSN modelling: the easier condensation on grains of HDO at low temperatures (active in the atmosphere of Earth and Mars, Bertaux & Montmessin 2001), and the smaller photodissociation rate of HDO than H_2O by solar UV (Cheng et al. 1999). Another potential fractionation mechanism is the production of an HDO molecule when an OH radical reacts with a D atom at the surface of a grain (heterogeneous chemistry), due to the preferential sticking of D atoms versus H atoms on grains.

4 DIFFUSE INTERSTELLAR BAND CARRIERS AND VERY SMALL INTERSTELLAR GRAINS

4.1 DIB observations and potential carriers

The DIBs represent more than 500 irregular weak absorptions in optical and near-IR stellar or galaxy spectra. For recent reviews and wavelength lists, see e.g. Sarre (2006), Hobbs et al. 2009, and the proceedings of the IAU297 symposium (Cami & Cox 2014). Their IS nature has been demonstrated by their correlations with the other parameters characterizing the IS gas and dust amount, in particular H columns and the colour excess $E(B-V)$ [B and V are the blue and visible magnitude of the star, $E(B-V)$ measures the differential extinction by dust between two wavelengths B blue and V visible, linked to the integrated dust column along the line-of-sight (LOS) to the star]. However, surprisingly all types of negative to positive correlations with molecular hydrogen have been found (Friedman et al. 2011; Lan, Ménard & Zhu 2015). According to observed DIB properties and correlations, DIB carrier candidates should primarily be sought among carbon-based organic molecules. Many arguments favour molecules in the gaseous phase and not dust grains, in particular the absence of polarization, the asymmetric and stable spectral profiles and more generally the fact that absorptions do not correspond to solid-state transitions in dust grains, although molecules adhering to dust grains are not totally precluded as carriers (Snow & Destree 2011). Due to the large number of observed bands, many different complex molecules could be involved.

No firm identification of a DIB carrier has occurred despite decades of observations and laboratory experiments, with the exception of the assignment of a pair of near-infrared DIBs to ionized fullerene C_{60}^+ (Foing & Ehrenfreund 1994) that was confirmed recently with laboratory gas phase experiments through helium tagging (Campbell et al. 2016). Despite this first identification, fullerenes cannot be responsible for all DIBs (Omont 2016) and other candidates must be identified. For many years, ionized PaHs were recognized as reasonable candidates (Crawford et al. 1985; Léger & d'Hendecourt 1985; van der Zwet & Allamandola 1985), and carbon chains or H_2 have also been considered, but studies were not able to definitely identify any carrier of this type (e.g. Salama et al. 2011). In the frame of his recent THEMIS evolutionary dust model, Jones (2014, 2016) proposed that DIB carriers are produced by photoprocessing and fragmentation of very small hydrogenated amorphous carbon grains produced around evolved stars or via accretion in molecular clouds and may be of two types: (i) UV-protected hetero-cyclic substructures within nanoparticles giving rise to the broad, UV-insensitive DIBs, and (ii) isolated dehydrogenated, radical, ionized, hetero-cyclic polyatomics giving rise to UV-sensitive DIBs. This close relationship between very small organic grains and DIB carriers is particularly important in the context of our discussion about relevance to comets.

4.2 Abundance variability of DIB carriers in response to the interstellar radiation field

It has been well established that one of the main physical parameters governing the DIB is the UV radiation field. Internal parts of a dense molecular cloud protected from the UV ionization on the one hand, and cloud ionized outer envelopes on the other hand correspond to very different DIB relative strengths, the so-called skin effect (e.g. Krelowski & Sneden 1995; Cami et al. 1997). Indeed, a recent Principal Component Analysis study by Ensor et al. (2017) has revealed a whole hierarchy of DIBs with respect to this radiation field/ionization criterion. As a well-known example, the 5780 Å DIB is strongly favoured in unshielded, ionized envelopes of the clouds and decreases deeper in the clouds, while the 5797 Å does not display such a strong decrease in the denser, radiation-protected regions. Therefore, the ratio between these two strong DIBs is a particularly good tracer of the exposure to the radiation field (e.g. Van Loon et al. 2009; Vos et al. 2011; Smith et al. 2013) and may be used as a proxy for the mean ionizing field. Since the UV field decreases from the low-density envelopes to the dense cores, the ratio is also a probe of the compactness of the encountered medium. In the case of a specific cloud, this can be seen schematically as the impact parameter of the LOS, small when it crosses the cloud in its centre, large when it crosses its ionized envelope. More recently, Ensor et al. (2017) and Elyajouri et al. (2017) found that the 6283 Å DIB is even more favoured in high radiation conditions than the

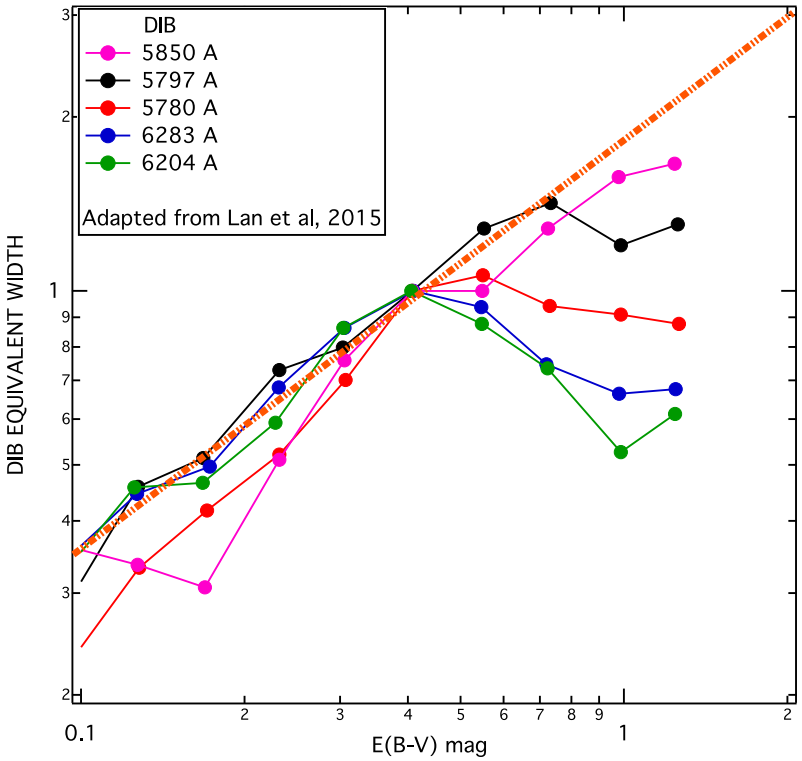

Figure 4. Average DIB EW as a function of the colour excess along the line of sight, for five strong DIBs. The data are taken from fig. 8 of Lan et al. (2015). All curves have been scaled to EW = 1 at $E(B-V) = 0.40$. The dash–dotted line serves as a guide to visualize departures from linearity above this colour excess value. The 'ionized' DIBs start to deviate from proportionality to the dust column at a lower colour excess compared to the 'neutral' 5797 and 5850 Å DIBs (see the text). However, even the most 'neutral' DIB 5850 Å stops following the reddening.

5780 Å DIB, i.e. the ratio 6283/5797 is an even better measure of this impact parameter. In the following section, we will use the 6283/5797 ratio to represent the envelope-to-core transition.

4.3 DIB saturation in cloud cores

In addition to the differentiated response of the various DIBs to UV shielding, it has been observed that at high reddening the strength of some DIBs stops increasing with extinction (Snow, Zukowski & Massey 2002b). Indeed, there are a few extreme cases of particular LOSs to stars with strong dust extinction [e.g. HD62542 with $E(B-V) = 0.35$] in which the main strong DIBs become very small with respect to the reddening and even become undetectable (Snow et al. 2002a). On the other hand, in a deeper study of this sightline, Adamkovics, Blake & McCall (2005) showed that most of the weak, so-called C2 DIBs known for being associated with dense molecular cores (and C2 absorption lines) are detected, confirming their potentiality as core diagnostics. However, we note that among the 15 C2 DIBs identified by Thorburn et al. (2003), which are either detected or have been given an upper limit towards HD62542, 12 have equivalent widths (EWs) [or upper limits] significantly below the levels reached towards the two other targets of reference in Adamkovics et al. (2005) after appropriate scaling to the reddening. Only the three 'blue' and very weak DIBs at 4363.8, 4734.79 and 4969.24 Å have a strength compatible with proportionality with the extinction. Therefore, in such dense clouds, globally the very large majority of DIBs level off with respect to the reddening or stop increasing linearly with the reddening. One simple and likely explanation for the lack of DIBs is that all ionized DIB carriers have been neutralized, and have agglomerated together with all neutral DIB carriers, forming a solid phase of organic material that cannot produce any molecular absorption. If this happens in existing molecular clouds, it may have happened also in the molecular cloud from which our Solar system was formed, suggesting the relevance with respect to organic matter in comets.

We wish to present further evidence of agglomeration of DIB carriers in dense clouds. Recently, Lan et al. (2015) exploited a large number of observations acquired with the massive Sloane Digital Sky Survey (SDSS) survey. Due to the selection of observations of stars at high Galactic latitude, the path lengths through the thin Galactic dust and gas layer are short and subsequently the sightlines cross very few molecular clouds, if any. For example, among the observations a significant level of extinction corresponds most of time to the crossing of only one single dense cloud (mono-cloud observation). This is contrary to most of the DIB studies of highly reddened stars at low Galactic latitude: in this latter case, the sightlines are entirely contained within the thin disc and a large extinction is generally produced by the Galactic matter spread along the LOS (the multicloud case). For ∼20 different DIBs, Lan et al. (2015) considered separately all LOS with the same extinction, and they averaged the EWs over all stars within each extinction bin to get plots of the DIB EW as a function of extinction. Some of the EW curves from Lan et al. (2015) are reproduced in Fig. 4, normalized to 1 for a colour excess $E(B-V) = 0.4$. It is clear that EWs of these mono-cloud observations all start to increase proportionally with extinction (measured by the colour excess). They then either keep increasing but no longer linearly with the colour excess $E(B-V)$, like in the case of DIB 5850 Å; level-off (saturate) above $E(B-V) \approx 1$, like DIBs 5780 and 5797 Å, or level-off then begin to decrease

as in the cases of DIBs 6204 and 6284 Å. Interestingly, a careful inspection of the Lan et al. (2015) results show that for all DIBs, including those like DIBs 4502, 4728, 5540 and 5850 Å which keep increasing up to high $E(B-V)$s, there is a threshold in the reddening above which the DIB strength stops following it. Having in mind that the LOS crosses a single cloud, we may assign large extinctions to LOS crossing the centre of a cloud, while more modest extinctions suggest LOS crossing more external parts of a cloud. This must be true on the statistical basis of the Lan et al. (2015) work. In agreement with the established hierarchy discussed in the previous section that is associated with the ionization, the departure from proportionality to the reddening is observed to start at a lower reddening level (i.e. in more external parts of the clouds) for those 'ionized' DIBs that are favoured in unshielded cloud envelopes, and at a higher opacity for 'neutral' DIBs. For example, the 6283 Å 'ionized' DIB starts to decline already at $E(B-V) \approx 0.4$, while the 5797 Å 'neutral' DIB follows $E(B-V)$ until $E(B-V) \approx 0.5$–0.6 and starts to saturate above this value. But, again, figures 8 and 9 from Lan et al. (2015) show that not only the 'ionized' DIBs, but also the 'neutral' DIBs tend to stop increasing with the reddening or level off in cloud central regions, i.e. the reddening-normalized DIB strength [the ratio between the DIB and $E(B-V)$] decreases in dense cores. This effect has been somewhat overlooked, and one of the reasons is that it is not observed when one uses observations of low-latitude, highly reddened individual targets (see fig. 8 of Lan et al. 2015). We argue that this is due to the fact that in those latter cases the reddening builds up in more than one cloud. Because the clouds can certainly not all be crossed at the same distance from their centres, i.e. all within their envelopes or all in their central cores, the cumulative reddening due to the intervening clouds is generated in regions with different physical conditions and DIB relative abundances. This has the effect of 'blurring' the trends associated with the cloud opacity revealed in the SDSS study. At variance with this situation, the Lan et al. (2015) sightlines most of the time cross only one single dense cloud that contributes to most of the absorption. In other words, the information on the link between the reddening and the DIB carrier abundance (reflected in the DIB strength) that is present in the 'mono-cloud' Lan et al. (2015) data is lost for the 'multicloud' cumulated $E(B-V)$. An additional study (not shown here) reveals the same difference in the case of the link between the reddening and the 6283–5797 Å DIB ratio.

We suggest that these recent observations of DIB decrease of slope, levelling-off or decrease in cloud dense and UV- shielded cores and of the decrease or disappearance of DIBs in some LOS like the one to HD 62542 are simply due to the fact that in the dense cores the DIB carriers do not exist in the same large quantities but instead start to make part of a solid phase of organic material, their 'parent' material. This is in agreement with the model of Jones (2016) and DIB carrier production by fragmentation of very small carbon grains. As noted by Jones (2016) 'if the DIBs are, as we propose.., due to nanoparticles and smaller, then there is a clear environmental explanation as to why they do not associate with the molecular hydrogen in the denser IS gas. This is due to the evolution of the dust properties' in these regions where the dust has accreted mantles of a-C: H and has been coagulated into aggregates. Here, all the small DIB-carrying nanoparticles have been swept up into larger structures in which their electronic transitions are submerged by the global, aggregate dust optical properties. One consequence of such a DIB origin is that if small IS carbonaceous grains are preserved in the solid phase of comet nuclei, then this phase contains the DIB carriers, either initially free or agglomerated onto grains or coagulated, and also similar molecules producing no detectable absorption (no-DIB organic molecules, such like C_{70}). Therefore, in our proposed scenario, the solid organic material of the comet contains a significant quantity of agglomerated DIB carriers. The COSIMA TOF-SIMS dust analysis is fragmenting these large molecules and only small fragments are recorded, but they are the sign of the existence of much larger organic molecules (Fray et al. 2016).

4.4 DIB disappearance versus very small grains increase

In addition to an extensive compilation of DIB data, Xiang, Li & Zhong (2017) have parameterized, when available, the corresponding optical–UV reddening law. Fig. 5 (bottom) displays their coefficient c4 that traces the far-UV (FUV) slope of the spectral reddening law as a function of the 'neutral' to 'ionic' DIB ratio $R = 5797/6283$ for more than 80 sightlines. A clear positive correlation is obtained. This correlation is not due the amount of dust that would act as a 'hidden' intermediate parameter, since, as shown in the figure, targets with very different reddening levels contribute to the trend. A close inspection shows that the positive correlation is due to the existence of two regions: at low R values, one finds a large dispersion of the UV slope, while above $R \sim 0.15$–0.2 only high values are present. Such a positive correlation, this time between the 5797/5780 DIB ratio and the 1300–1700 Å reddening law gradient was previously found by Megier et al. (2001). Since the FUV rise is known to be linked to the increase of VSGs, these authors suggested that the 5797 Å DIB carrier is easily destroyed by the UV field and protected by the FUV absorbing dust, or that its carrier needs catalysis by VSGs in order to grow. However, the 5797 Å DIB carrier destruction in envelopes is very likely not at the origin of the evolution of the ratio, since this carrier follows the amount of dust up to $E(B-V) = 0.4$. Instead, it is the disappearance of the 5780 Å DIB carrier in cloud cores that drives the ratio, as shown by the strong levelling-off of DIB 5780 Å in dense areas (see e.g. Ensor et al. 2017). Contrary to the interpretation of Megier et al. (2001), we suggest that the correlation between the 5797/5780 (or $R = 5797/6283$) DIB ratios and the FUV rise is simply explained by the simultaneous disappearance of the DIB carriers and apparition of VSGs, due to the coagulation of the former to make part of the latter. On the other hand, DIB carriers disappear in very strongly irradiated tenuous media far from dense clouds through photofragmentation, as observed in Photo Dissociation Regions, which results in DIB carrier peak abundances in cloud external parts.

In support of our hypothesis, an additional comparison is shown in Fig. 5, between the FUV rise discussed previously and the 5797 Å DIB disappearance observed by Lan et al. (2015). Here, again this 'mono-cloud' data set utilises DIB strength normalized to the reddening to investigate the evolution of physical properties from cloud centres to their envelopes. It can be seen (Fig. 5, top) that at low $R = 5797/6283$ Å ratio, the normalized DIB increases with R (for LOS crossing the cloud from outer envelopes to deeper regions) that is in agreement with maximum DIB abundance in external parts of the clouds as discussed above. Above a ratio $R \sim 0.15$–0.2 the DIB strength starts to decrease strongly with the amount of dust, exactly at R values for which the rise in FUV, again represented by the c4 index, becomes systematically strong.

There are hints that other DIBs stop growing in proportion with the reddening in sightlines characterized by a strong FUV rise in the extinction curve. Fig. 6 shows the DIB EW normalized to the reddening as a function of the FUV rise index c4 for three other strong DIBs, in addition to DIB 5797. The data are again taken from the Xiang et al. (2017) compilation. Since most sightlines cross

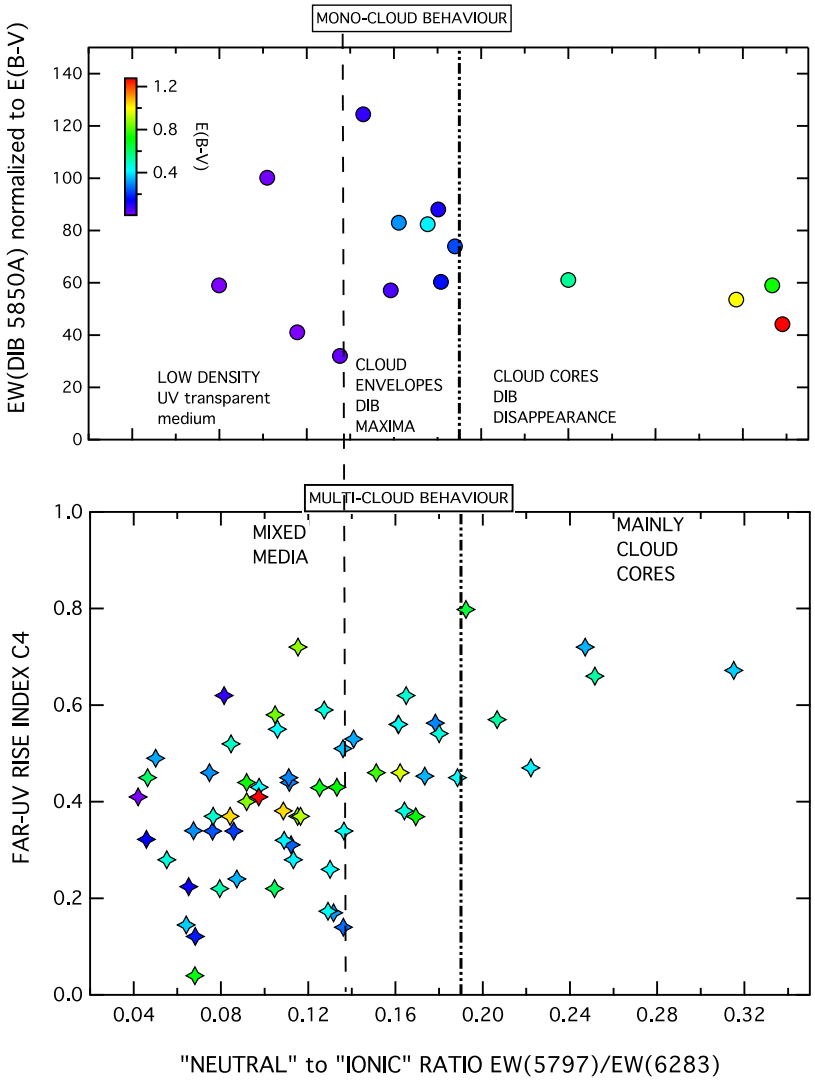

Figure 5. Top: 'Saturation' of the 'neutral' DIB 5797 Å in SDSS data as a function of the 5797–6283 Å DIB ratio R used as a 'radiation-shielding index'. DIB strengths and reddening $E(B–V)$s are taken from Lan et al. (2015). Above $R \sim 0.15 – 0.2$, the DIB starts to level-off with respect to the reddening. This is also associated with a strong increase of $E(B-V)$ (colour scale). Bottom: FUV rise index of the reddening curve known to be associated with VSGs VSGs as a function of the same 'radiation-shielding' index R. DIB strengths and C4 indexes are from the DIB compilation and reddening law parameterization of Xiang et al (2017). Here, large values of R are not necessarily associated with high $E(B-V)$s since more than one cloud contribute. Below $R \sim 0.15$, there is no clear trend for the FUV rise. Above $R \sim 0.15$, the FUV rise is very strong. The similarity between this rise and the strong saturation observed in Lan et al. (2015) data versus the same shielding index suggest that the two phenomena are linked, i.e. VSGs appear when DIB carriers disappear and reciprocally.

multiple clouds, this approach results in more complex and 'blurred' relationships. However, despite the large data point dispersion due to the existence of several clouds along the sightlines, at large values of c4 (c4 $>$ 0.7) the normalized DIB strengths are lower than the maximal values reached in the cloud envelopes, and this is observed for the four DIBs, including the 'neutral' DIB 5850 Å. Such relationships should be investigated for more DIBs, especially the C2 DIBs that are known for being relatively abundant in dense cores. Unfortunately, the number of measurements of these very weak DIBs is still too small to facilitate reliable statistical studies. Future data sets of high quality are crucially needed to study further those bands. For the moment, we retain the results obtained for the relatively strong DIBs.

Our main point here is the following: if the DIB carriers coagulate in dense clouds to be part of small grains, such coagulation of the DIB carriers (and their undetected counterparts, the 'no-DIB' molecules) in the form of substructures in very small organic dust grains in high-density clouds must also have been possible in the protosolar nebula. In the cold, outer regions of the nebula, the grains may have aggregated 'gently' in the hierarchical process from grains to pebbles to cometesimals as described by Davidsson et al. (2016), and still be present in the cometary nuclei, pristine and preserved, and still containing the DIB carriers and similar large organic molecules.

4.5 Carbon inventory of DIB carriers, fullerenes and PaHs in the ISM

We consider the organic carbon inventory in the ISM in the following approximate manner. Inorganic material is mainly contained in large dust grains with silicate cores manifesting themselves by IS extinction of star light, larger in the blue than in the red in the optical part of the spectrum. As presented above, the differential extinction is classically referred to as the colour excess $E(B-V)$, where B and

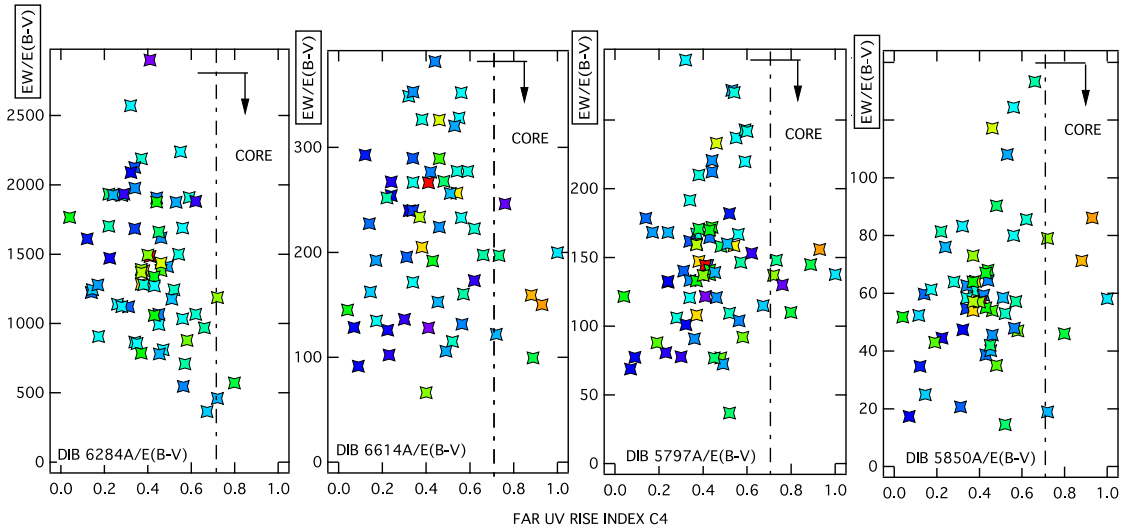

Figure 6. DIB EW normalized to the reddening as a function of the FUV rise index c4 for four different DIBs (compiled DIB data and fitted c4 coefficients are from Xiang et al. 2017). When c4 reaches high values (>0.7, high fraction of VSGs) normalized DIBs are below the maximal values reached at lower c4 coefficients. Note that the maxima occur at increasing values of c4 from ∼0.35 to ∼0.65 for DIBS 6284, 6614, 5797 and 5850A, respectively, reflecting each different type of 'skin effect'.

V are, respectively, blue and visible magnitudes of the star. This colour excess can be roughly scaled to an IS hydrogen column of 5×10^{21} H atoms cm^{-2} when $E(B-V) = 1$. The dust/H mass ratio in the ISM is classically estimated to be 10^{-2}.

For an estimate of the mass abundance of organic material in the DIB carriers, we start using the only reliably identified absorption features at 9577.5 Å (and three other nearby lines) of C_{60}^+, for which an absorption cross-section was measured in the laboratory and corresponding lines identified in IS absorption (Foing & Ehrenfreund 1994; Campbell et al. 2016). In particular, observations toward the reddened star HD 183143 for which the reddening $E(B-V) = 1.27$ leads to a column density of $(2 \pm 0.8) \times 10^{13}$ cm^{-2} of C_{60}^+ (Campbell et al. 2016), and a total column density of C atoms of 1.2 10^{15} cm^{-2}. When compared to the carbon cosmic abundance [C]/[H] of 5.2e $\times 10^{-4}$, it means that a fraction 3.6×10^{-4} of all carbon atoms of the ISM is locked to C_{60}^+ for this particular LOS. This estimate is totally in line with an average estimate on 17 stars LOS of $(4 \pm 2) \times 10^{-4}$ of carbon locked in this ionized fullerene molecule (Omont 2016).

We extend the computation above related to C_{60}^+ to produce a more refined estimate of the mass of carbon contained in the DIB carriers, which relies on the observed DIBs absorptions and their analysis by Hobbs et al. (2009). They found 489 DIBs spread between 4000 and 8800 Å in the LOS to HD 183143. For each of the DIB, they measured their central wavelength, their full width at half-maximum (FWHM) and their equivalent width of absorption EW (in mÅ). Knowing the oscillator strength f_{os} of an observed DIB transition, the number of the DIB carrier molecules (integrated along the LOS) producing a particular DIB may be related to the measured equivalent width EW. The definition of the oscillator strength f_{os} of a transition is related to the cross-section for one molecule σ_ν (in cm^2) integrated over all frequencies (in cm^2 hz):

$$\int_0^\infty \sigma_\nu d\nu = \frac{\pi e^2}{m_e\, c}\, f_{os}. \quad (3)$$

Then, the oscillator strength f_{os} may be related to the carbon abundance and the equivalent width EW, expressed in mÅ per unit of $E(B-V)$, in short in mÅ mag^{-1}. It can be written as (e.g. Cami 2014; Omont 2016)

$$\mathrm{EW}\left(\mathrm{m\AA\ mag^{-1}}\right) = 10(\lambda/5500)^2(f_{os}/10^{-2})(X_{CM}/10^{-4})\,(60/N_C), \quad (4)$$

where λ is the wavelength in angströms, N_C is the number of carbon atoms in the molecule and X_{CM} is the fraction of IS carbon locked up in the considered type M of the molecule. The typical values $f_{os} = 10^{-2}$ and $N_C = 60$ are proposed in Cami (2014), and we just take these proposed typical values as average values. As noted in Omont (2016), X_{CM} refers to the total carbon abundance in the ISM including solids, assumed to be $N_C/N_H = 3.9 \times 10^{-4}$.

The EWs of all DIBs are to first order correlated with the quantity of matter (related to star reddening) along the LOS to a star. For our calculation, we postulate that each DIB must be assigned to a different carrier/molecule. If a particular molecule were producing two different DIBs at two different wavelengths, then the EW of these two DIBs would be perfectly correlated to all stars (like the two IS sodium lines D_1 and D_2). Indeed, it has been verified (at least for the most intense DIBs) that one particular EW of a DIB is not perfectly correlated to any other DIB, showing that most of DIBs, if not all, are the signature of different molecules. There is of course the notable exception of the two DIBS of C_{60}^+, at 9632.7 and 9577.5 Å, and the unique quasi-perfect correlation of DIBs 6196 and 6614 Å (McCall et al. 2010).

Considering that these are exceptions, we may apply formula (4) to all the reported DIBs, to get the value X_{CM} for all molecules. We have done this exercise assuming a mean value of $f_{os} = 0.01$, and a mean value of 60 carbon atoms per molecule producing a DIB. These values are assumed to be typical averages. For comparison, the number of carbon atoms is obviously 60 for C_{60}^+ and the oscillator strength is 0.025 ± 0.008 for the two main lines of C_{60}^+ (Campbell et al. 2016). SOMs are rapidly destroyed by UV-EUV in the diffuse ISM and only species with more than 50 carbon atoms are likely to survive (Jones 2016 and references therein). Fig. 7 is the histogram of all values of X_{CM} estimated in this way, derived from the table of EW for all DIBs recorded by Hobbs et al. (2009).

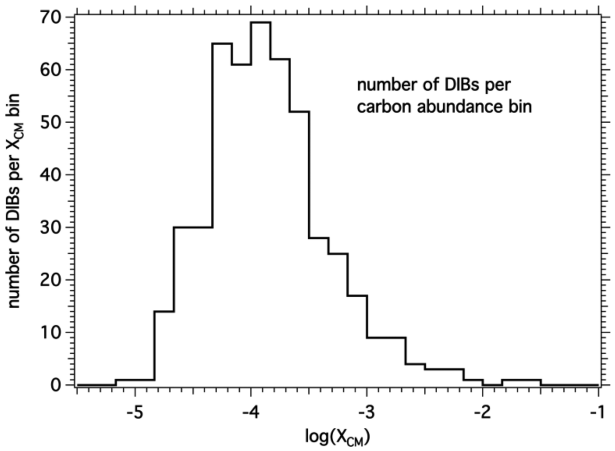

Figure 7. Histogram showing the number of absorption features (DIBs) per bin of estimated values of log(X_{CM}) where X_{CM}, the fraction of IS carbon locked in molecule M, comes from formula (4), applied to all DIBs from the table of EW for all DIBs recorded by Hobbs et al. (2009).

The largest DIB in absorption (at 4428.83 Å) is responsible for 2.9 per cent of total carbon, and the second largest (at 6284.28 Å) for 1.9 per cent. When all values of X_{CM} are added together, it is found that at least 20 per cent of IS carbon is locked up in a DIB carrier. This is a minimum value, because to this estimate, we should add all DIBs recently measured in the near infrared (0.9 to 1.5 μm). We have compiled the values of EW(mÅ mag^{-1}) for 25 DIBs in the IR, from 9880 to 16,585 Å in the literature and in our own data. The strengths of the main DIBs were taken from Hamano et al. (2016, 18 DIBs from 9880 to 13,175 Å) and Zasowski et al. (2015, 15,273 Å, the DIB from ground-based APOGEE monitoring programme). The strengths of weak DIBs in APOGEE spectra are taken from table 2 and fig. 5 of Elyajouri et al. (2017). We found an additional 10 per cent of total carbon when applying the formula (4) to these IR DIBs and we will retain for further calculations an approximate value of 0.30 for the fraction of IS carbon atoms that are under the form of large organic molecules in the ISM, showing up as a DIB in absorption.

Our calculation is admittedly rather uncertain, in the absence of measurements of f_{os} values (except for C_{60}^+); it is clearly larger than other estimates found in the literature, but on the same order than some others. For instance, Tielens (2013) estimated the same parameter at 0.002, assuming that the PaHs are the potential carriers of DIBs. This estimate was based on the assumption that the oscillator strength is $f = 0.01$ for *each atom* of carbon of the DIB carrier. Much larger estimates are also found, showing at least the degree of uncertainty on this parameter. Dwek et al. (1997) estimated that the fraction of cosmic carbon locked up in PaH molecules is 20 per cent, with similar estimates in Joblin et al. (1992). Assuming that PaHs will contribute to the DIB carriers, this estimate corresponds to the same order of magnitude as ours. In the case of the buckminsterfullerene C_{60}^+ the total oscillator strength is 0.025 ± 0.008 for the two main lines of C_{60}^+ (Campbell et al. 2016), implying a much lower strength per C atom than for PaHs. Using this example of C_{60}^+ and assuming that each carrier produces four bands, Jones (2016) found $X_{CM} = 0.06$ for a total of 100 carriers.

Of course this does not preclude the existence in the ISM of other large organic molecules that do not exhibit any DIB absorption feature: the no-DIB (organic) molecules. For example, a DIB carrier may be an ionized molecule, like C_{60}^+, while the neutral form does not show a DIB. This is supported by the strong links of DIBs with the radiation field (Cami et al. 1997, 2010; Friedman et al. 2011; Vos et al. 2011; Ensor et al. 2017), the fact that PaHs and in general large organic macromolecules get easily ionized (e.g. Montillaud, Joblin & Toublanc 2013; Tielens 2013), and the formation of cluster cations after dehydrogenation of such molecules in a strong UV field (e.g. Jones 2016). Vice versa, some DIBs might be produced by a neutral form and decrease in ISM regions with strong UV illumination ionizing the molecule, with no further DIB production.

5 COMPARISON OF ORGANIC MATTER ABUNDANCE IN THE ISM AND IN COMETS

Before discussing quantitatively the organic matter itself, we set the stage by summarizing the situation of the abundance of carbon element C both in comets and the ISM.

Table 2. First four columns: atomic number Z, name, atomic mass and mass fraction of the main elements in the Galaxy and ISM in ppm units.

1	2	3	4	5	6
Z	Element	Mass (amu) of main isotope	Mass fraction in Galaxy and ISM (ppm)	Relative Mass Fraction in ISM, Organic (ppm)	Relative Mass Fraction in ISM, Mineral (ppm)
1	H	1	739 000		
2	He	4	240 000		
6	C	12	4600	1380	
7	N	14	960		
8	O	16	10 400		1486
10	Ne	20	1340		
12	Mg	24	580		580
14	Si	28	650		650
16	S	32	440		440
26	Fe	56	1090		1090

Notes. Column 5: estimated relative mass fraction of Organic DIB carriers in ISM (C is kept, H and other elements are neglected). Column 6: relative mass fraction of element in the mineral component of ISM in the same units as in column 4. Only a fraction of oxygen is present, with all Mg, Si, S, Fe assumed to be in minerals, and other elements neglected. The mass ratio of organic/minerals comes to $R_{ISM} = 0.32$.

5.1. Carbon abundance inventory in cometary dust

At present, the best determination of the elemental composition of cometary dust comes from the PUMA 1 instrument during the Vega 1 fast encounter with Halley's comet in 1986, as reported by Jessberger, Christoforidis & Kissel (1988). The 79 mass spectra of individual particles obtained in the non-compressed mode (mode 0) are the most reliable, and were used to compare the elemental composition to the CI reference. CI is a carbonaceous chondrite of type Ivuna whose composition is considered as a proxy of solar or cosmic element abundances, except for C and some other volatile elements. Taking the abundance of Mg as a reference, it was found that the ratio of C/Mg was 11 times larger in the comet dust than in the CI composition reference (Jessberger, Christoforidis & Kissel 1988). However, it is well known that the CI composition reference is strongly depleted in carbon with respect to solar/ISM composition (as may be computed from Lodders & Palme 2009). Taking the elemental compositions of solar and CI reference in Lodders & Palme (2009), we find that the PUMA ratio of C/Mg is 1.16 ± 0.23 times the solar ratio (6.98), which means that the comet abundance of carbon relative to Mg is indeed ∼solar, which is also the assumed composition of the ISM at large. For the mineral-forming elements Si, Mg and Fe, Halley's comet dust particles have the same element composition as CI and solar, which do not differ much from each other for these elements (Jessberger, Christoforidis & Kissel 1988).

5.2. Distribution of Carbon element into various reservoirs in the ISM

We first list the various reservoirs of carbon atoms identified in the ISM:

(1) the atoms (and some C^+ ions and di-atomic molecules C_2, CH) in the gas phase, revealed by their atomic/diatomic absorption lines;
(2) SOMs identified through their microwave transitions (e.g. CH_3 CNO, methyl isocyanate, etc.);
(3) large dust grains (solid phase) composed primarily of minerals;
(4) small carbonaceous (carbon-rich) grains;
(5) large organic molecules that are detected from their DIB absorption features (including PaH): the DIB carriers;
(6) similar large organic molecules that do not have observables transitions: we may call them no-DIB molecules.

The first two reservoirs are in the gas phase and/or volatile, and are ignored in the following as irrelevant to the composition of cometary dust (though they are of course very relevant to the volatile part of the comet, detected in the gaseous cometary coma).

For the ISM dust reservoir no. 3, we could think of a carbonaceous mineral like CO_3Ca (calcium carbonate). There has been recently a quite interesting progress in the knowledge of the composition of IS dust (Altobelli et al. 2016). The Cosmic Dust Analyzer (CDA) Instrument onboard *Cassini* spacecraft provided the atomic composition of 36 IS grains [Inter Stellar Dust (ISD)] in the mass range 5×10^{-18} to 10^{-16} kg (Altobelli et al. 2016). The ISD are identified as IS from their velocity vector (magnitude and direction), and their composition is determined with a TOF spectrometer after vaporization and ionization upon impact on a target of Rhodium. Overall, it is found that Mg/Si, Fe/Si, Mg/Fe and Ca/Fe atomic ratios are on average CI chondritic. There is a small C^+ peak in the TOF spectra, but most of it may be assigned to a known contamination from the Rhodium target (Altobelli et al. 2016). Most likely, the depletion factor C/O and C/Mg is 10 or more, with respect to the CI reference. Since the CI reference is already depleted in carbon with respect to solar by a factor of ∼10, it shows that the mineral IS dust particles detected by CDA are almost void of carbon.

However, only large grains can be detected in the heliosphere. Small grains (∼200 nm size or less) become easily electrically charged, which are deflected by the solar wind and leave the IS flow penetrating the Solar system. If small carbonaceous (carbon-rich) grains (200 nm size) are an essential component of carbon carriers, as in the theoretical description of Jones, and do exist in the Local IS cloud presently encountered by the Sun, they could not be detected by CDA/*Cassini*. Therefore, the *Cassini* results on the absence of carbon imply that most of the ISM carbon must be in the three remaining reservoirs 4 to 6.

During the PUMA/PIA investigation, one comet dust particle (out of several hundreds) composed of almost pure carbon was indeed detected, showing a remarkable isotopic ratio of $^{12}C/^{13}C$ ratios as high as 5000 (Jessberger & Kissel 1991), linking cometary matter to certain circumstellar graphite grains extracted from carbonaceous chondrites (Anders & Zinner 1993). But this was a unique event, and it is likely that pure small carbon grains are not, in the comet, a large reservoir of carbon. The reservoir 5 is discussed in the next subsection.

5.3 Relationship between locked carbon and organic/mineral mass ratio in the ISM

In Section 4.5, we have made a quantitative assessment of the fraction of ISM carbon that could be locked in into large organic molecules producing DIB absorption features (the DIB carriers, reservoir no. 5) and found this fraction potentially as high as $F_{\rm DIB} = 0.3$.

The estimate of the organic to mineral mass ratio $R_{\rm ISM}$ in the ISM proceeds as follows. We use values of mass ratios of the most important elements in the Universe (Table 2) and assume they are valid for the ISM composition to first order. The mass of organic carbon which shows up as DIBs is 0.3×4600 (from column 3 of Table 2) and we neglect other lighter atoms H, O, N in the mass budget of organic material (column 4). The case of oxygen atoms, whose mass fraction is the most important after the light elements H and He, must be treated separately, because one part of oxygen atoms will be under the form of minerals in the comet, and one part will be under the form of ices (H_2O and CO_2). For metals and sulfides, we take the elemental fractional masses of column 3 for Fe (representing metals) and sulfur for sulfides with no modification. We take SiO_4Mg_2 as representative of silicates, and assume no O atoms in metals and sulfides. Therefore, the mass of O atoms locked in minerals is in proportion of the mass of Si, $(64/28) \times 650 = 1486$ placed in Column 5. The mass ratio of organics to minerals is obtained by dividing the organic carbon mass (again neglecting H and other elements) by the sum of O, Mg, Si, S and Fe in column 5. The result is $R_{\rm ISM} = 0.32$. It is a pure numerical coincidence that $R_{\rm ISM} = 0.32$ is almost identical to $F_{\rm DIB} = 0.3$, but this may serve as a rule of thumb, since both numbers will scale together.

5.4 The mass ratio organic/mineral $R_{\rm C}$ in cometary dust

From a thorough analysis of all the data collected by PUMA-1 and PUMA-2 instruments, it was found that the overall mass ratio of silicates to organics in Comet Halley dust is between 2 and 1 (Fomenkova 1999). By adding to silicates the contribution of S

and Fe from column 6 of Table 2, the ratio of silicates to organics between 2 and 1 yields a ratio R_C of organics to minerals in the cometary dust $0.32 < R_C < 0.64$.

During the two years at the comet, the COSIMA instrument onboard *Rosetta* collected at low velocity more than 31 000 particles, released from 67P/CG before and after the comet's perihelion. About 250 particles, ranging from ∼50 to ∼1000 μm in size, were analysed with the TOF-SIMS technique (Baklouti et al. 2017). The dust particles are void of ice, which had ample time to sublimate before collection and analysis by COSIMA, if there were any when leaving the nucleus. As reported by Baklouti et al. (2017), the collected dust is composed of ∼54 per cent of minerals, and ∼46 per cent of organic matter in mass. Therefore, the cometary mass ratio of organic/minerals is $R_C = 46/54 = 0.85 \pm 0.4$ (with a rather large error bar of ∼50 per cent according to the authors) in the non-volatile fraction of the comet. Here, we explicitly exclude H_2O and CO_2 from the discussion, because, as shown in the above discussion on the variable D/H ratio from comet to comet, there is strong evidence that H_2O ice (and a fortiori CO_2 ice) is not of IS origin, but rather was processed during the Solar system formation. Therefore, the value derived from COSIMA is $0.45 < R_C < 1.25$.

For further discussions and comparison with R_{ISM}, we take the average value of Halley/PUMA and C67P/CG/COSIMA findings, $R_C = 0.66 \pm 0.3$, the uncertainty encompassing both PUMA and COSIMA middle values.

5.5 Comparison between the organic/mineral mass ratio in cometary dust and in the ISM

Our estimates in Section 5.3 indicated that if the fraction of IS carbon locked into organic molecules is 0.30 then $R_{ISM} \sim 0.32$. This is to be compared with $R_C = 0.66$ estimated above. Both numbers are associated with very large uncertainties, and equality is not fully excluded. But, taken at face value, the mass ratio of organic material to minerals seems larger in comets than in the ISM by a factor ∼2. This would imply that a substantial fraction of the organic material found in the comet would have been fabricated during the formation of the Solar system. However, the alternate scenario in which all cometary organic material comes from the original ISM cannot be excluded either. First, our calculations of $R_{ISM} = 0.32$, based on EWs of DIBs are very uncertain and are assuming typical values of oscillator strengths that might be overestimated, yielding less carbon locked in the DIB carriers than reality. But, more importantly, a substantial part of IS carbon could be locked in small carbonaceous grains and large organic molecules, which do not absorb (or absorb enough) to produce a DIB, and are undetectable: the no-DIB molecules. This is the case for the neutral molecule C_{60}: only the ion C^+_{60} displays a DIB, while its neutral counterpart C_{60} does not. Also, the neutral molecule C_{70} has been detected via infrared emission (Cami et al. 2010), the spectrum of C_{70}^+ was obtained in the laboratory, showing a series of absorptions in the range 7372–7960 Å, but too weak to be detected through IS absorption (Campbell et al. 2016).

6 DISCUSSION AND CONCLUSIONS

We have discussed the observed diversity of $(D/H)_{H2O}$ ratio in comets in the frame of the most recent models of $(D/H)_{H2O}$. It is clear that the indirect isotopic exchange through neutral–neutral reactions implying, O, H, D, H_2, HD, OH, OD... is much more efficient than the direct isotopic exchange reaction between H_2 and H_2O in the gas phase (Yang et al. 2013). However, while Yang et al. (2013) explain the diversity of $(D/H)_{H2O}$ ratio in comets by a fast reset of $(D/H)_{H2O}$ to the IS value of $(D/H)_{H2}$, followed by subsequent vertical infall of HDO-rich water from the cloud nebula (new IS material) at various distances from the sun, we propose a simpler explanation: the observed radial gradient of $(D/H)_{H2O}$ may be obtained by a moderate radial mixing. The neutral-neutral reactions are happening near the sun, radial mixing will replace originally D-rich H_2O by D-poor H_2O produced near the hot central solar region, but this replacement will simply decrease with increasing solar distance because of moderate radial mixing.

We have argued that the observed diversity of $(D/H)_{H2O}$ ratio in comets excludes the scenario in which IS ice would have survived the formation of the Solar system up to inclusion in comet nuclei. Instead, a heating episode sublimating ice at least up to the distance of formation of comets is well described by current thermal models (Chick & Cassen 1997). In such models, the temperature in the region 10–30 au was high enough for a complete sublimation of IS ices, but stayed below ∼250 K letting the organic IS material to survive intact. The IS grains of the protosolar nebula may have lost their icy mantles but kept their carbonaceous grains. This is in total agreement with the scenario of gentle hierarchical accretion process proposed by Davidsson et al. (2016).

We have assembled and developed several arguments based on recent findings that favour the preservation of DIB carriers within the solid organic matter of comets suchlike 67P/CG. We showed that the organic to mineral mass ratio in the nucleus of 67P, $R_C = 0.66 \pm 0.3$, is about twice that of a crude estimate for the ISM ($R_{ISM} = 0.32$), taking into account the absorptions of all DIBs. One obvious way to 'fill the gap' is to include as parts of the cometary organic matter, the small IS carbonaceous grains and potentially a fraction of large organic molecules in the ISM that are not detectable in absorption because of lack of appropriate transitions. One known example is C^+_{60}, the ionized fullerene, which is detected, while the neutral counterpart cannot be detected but is certainly there. Another example is C_{70}^+ the transitions of which are too weak (Campbell et al. 2016).

A strong carbon depletion in IS dust grains flowing through the Solar system was recently discovered (Altobelli et al. 2016). At first sight, this result contradicts the above scenario. We propose a simple explanation for this carbon depletion in ISD grains: instead of being locked in the large grains detected onboard *Cassini*, most of the carbon in the diffuse ISM is part of the smaller carbonaceous grains and in large organic molecules. It is well known that small grains and particles are deflected by the solar wind out of the inner heliosphere and escape detection.

Some recent evolutionary dust models and observations of the ISM matter suggest that DIB carriers are UV-processed partially de-hydrogenated hetero-cyclic fragments of very small IS carbonaceous grains and are present at interfaces between the very compact icy cores of clouds and the surrounding low-density UV-irradiated medium. We presented evidence of this transformation based on the recent, numerous observations confirming the general disappearance of DIB carriers in cloud cores, and on the concomitance of the DIB carrier disappearance and a FUV steepening of the reddening curve, a steepening attributed to an increased number of VSGs.

There are very few papers discussing DIBs in the context of comets. We mentioned earlier the tentative assignment of one blue emission to a known particular band (A' Hearn et al. 2014). O'Malia et al. (2010) have attempted to detect the absorption of known DIBs in the coma of two comets without success, by observing stars through the comet. As discussed by O'Malia et al. (2010), one difficulty is to find a suitable star whose LOS has to pass very near

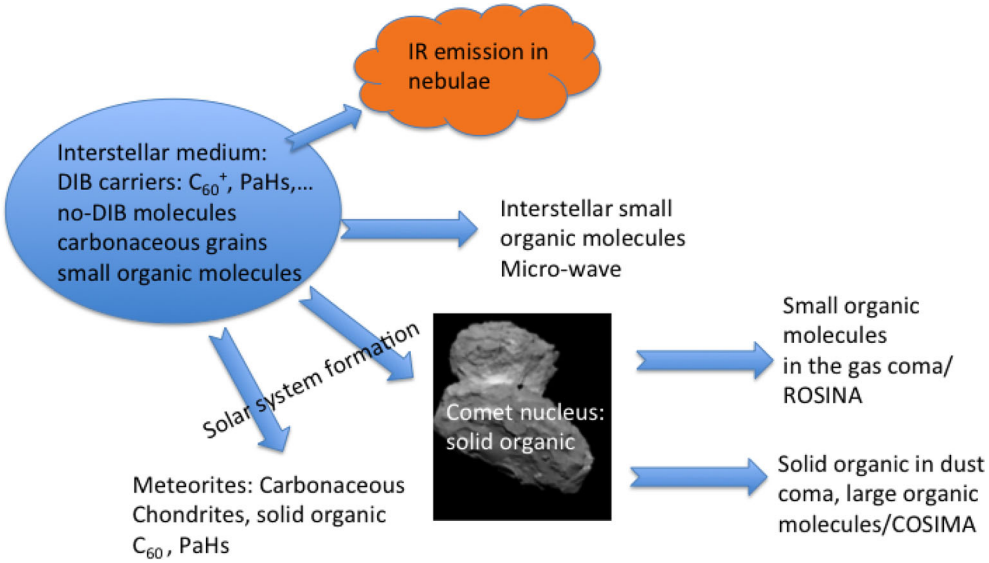

Figure 8. Schematic of the relation between cometary material analysed in the coma of 67P/CG by Rosina and COSIMA and components of the ISM. DIB carriers, PaHs, no-DIB molecules, carbonaceous grains, SOMs are found in the ISM, in the gaseous and dust coma of the comet and in some IR IS emission regions.

the nucleus of the comet (10^3–10^4 km), and rather bright. A signal to noise of ∼300 is required, corresponding to a 3σ DIB EW limit of 5 mÅ assuming an FWHM of 0.5 Å. A spectral resolving power of 38 000 would allow the emissions of rotational lines of C_2, C_3, CN, and other molecules to be resolved (O'Malia et al. 2010).

Though this technique is certainly worth pursuit in the future, it may also be the case that DIB carriers are only in the solid refractory phase, and therefore cannot absorb as they do when they are individually floating freely in the gas phase of the ISM.

Indeed, we are suggesting that the very organic molecules that are detected in absorption in the ISM, the DIB carriers (and likely other similar organic molecules undetected in absorption, the no-DIB molecules), have ended up in the nucleus of comets, either as free macromolecules or as envelopes of the small carbonaceous grains, thanks to the gentle hierarchical process of formation of cometary nuclei, and are still there. The ratio of organics/minerals in the comet of 67P/CG is about twice that of the same ratio $R_{\rm ISM}$ that we inferred on the quantitative basis of the observable DIB carriers. Though a massive fabrication of organic material in the early Solar system cannot be precluded by this existing gap, another simpler way to fill the gap is to invoke the mass contained in the small carbonaceous grains and in undetectable large organic molecules in the ISM, similar in structure and composition to the DIB carriers, like C_{60} and C_{70}^+. Following the Occam's razor principle claiming that the simplest explanation is the most likely, we would adopt this conclusion. In summary, organics in comets would be pre-solar (certainly at least ∼50 per cent), while water ice is not.

Processes that could reduce the ratio of organics/minerals during the long journey from ISM to comet nuclei are a strong heating destroying the organic molecules, either in the inner Solar system near the sun, or a radioactive heating within bodies larger than ∼200 km. Both processes are excluded in the comet nuclei formation scenario proposed by Davidsson et al. (2016), which evolves via gentle, hierarchical agglomeration scenario up to the present size of the nucleus, and the fact that we found $R_{\rm C} > R_{\rm ISM}$ is consistent with the absence of such a mechanism for comets. But it is clear that the heating destruction process of organics played a role for meteorites, debris of bodies formed in the inner Solar system, which are much poorer in organic abundance than comet 67P.

The connection between DIB carriers and comet nuclei increases substantially the scientific interest of a comet sample return mission. Once individual molecules are identified in the returned organic material of the comet through gas chromatography coupled to mass spectrometry (or other analytical methods), a synthesis of such heavy molecules could be used to measure their optical absorption properties as it was done for C_{60}^+ (Campbell et al. 2016), for a match with already known DIBs.

In this respect, it is important to note that this cometary organic material is refractory: it is robust to temperatures of 300 K at least. Therefore, the sample return capsule does not need to be maintained at cool temperatures to preserve ices, a technical requirement that increases considerably the cost of a comet sample return mission.

The early bombardment of the inner Solar system by comets is considered to have provided a large amount of organic material to the early Earth, from which life could have emerged. We already knew that atoms of our body heavier than lithium were fabricated inside stars through nucleo-synthesis. Now, there is evidence that IS molecules may have been a crucial progenitor of life in our planet through comet bombardment, and likely/perhaps in many other exoplanets in the habitable zone of their star, since DIB carriers are seen ubiquitously in our Galaxy and other galaxies as well.

Fig. 8 is a cartoon illustrating some relations between the ISM, the Solar system, comets nuclei and comae. The various components (PaHs, DIB carriers, SOMs, no-DIB molecules, carbonaceous grains) are seen in the ISM (blue ellipse), in particular IR emission regions (PaH in emission), and in gas and dust in the coma of comet 67P/CG.

ACKNOWLEDGEMENTS

JLB acknowledges the support of CNES through his participation to OSIRIS and ALICE investigations on *Rosetta* mission. RL acknowledges the support of Ministère de la Recherche through her ANR STILISM. We are grateful to Björn Davidsson for useful discussions, and to Michael A'Hearn (recently deceased) for his

positive appreciation of the manuscript at an early stage. We also wish to thank the anonymous referee for their numerous positive and helpful suggestions, and Matt Taylor for a careful reading of the manuscript.

REFERENCES

Adamkovics M., Blake G. A., McCall B. J., 2005, ApJ, 625, 857
A' Hearn M. F., Wellnitz D. D., Meier R., 2014, in Cami J., Cox N. L. J., eds, Proc. IAU Symp. 297, The Diffuse Interstellar Bands. Cambridge Univ. Press, Cambridge, p. 216
Altobelli N. et al., 2016, Science, 352, 312
Altwegg K. et al., 2015, Science, 347, A387
Altwegg K., 2016, ESA blog. Available at: http://blogs.esa.int/rosetta/2016/09/29/the-cometary-zoo/
Anders E., Zinner E., 1993, Meteoritics 28, 490
Baklouti D. et al., 2017, Asteroids, Comets, Meteors - ACM2017 – Montevideo
Becker L., Bunch T. E., Allamandola L. J., 1999, Nature, 400, 228
Bertaux J. L., Montmessin F., 2001, J. Geophys. Res., 106, 32879
Bertaux J. L., Blamont J. E., 1970, Comptes-Rendus de l'Académie des Sciences B, 270, 1581
Bieler A. et al., 2015, Nature, 526, 678B
Bockelée-Morvan D. et al., 1998, Icarus, 133, 147
Bockelée-Morvan D. et al., 2000, A&A, 353, 1101
Bockelée-Morvan D. et al., 2015, Space Sci. Rev., 197, 47
Cami J., 2014, in Cami J., Cox N. L. J., eds, Proc. IAU Symp. 297, The Diffuse Interstellar Bands. Cambridge Univ. Press, Cambridge, p. 370
Cami J., Sonnentrucker P., Ehrenfreund P., Foing B. H., 1997, A&A, 326, 822
Cami J.,, Bernard-Salas J., Peeters E., Malek S. E., 2010, Science, 329, 1180
Campbell E. K., Holz M., Maier J. P., Gerlich D., Walker G. A. H., Bohlender D., 2016, ApJ, 822, 17
Capaccioni et al., 2015, Science, 347, a0628C
Ceccarelli C., Caselli P., Bockelée-Morvan D., Mousis O., Pizzarello S., Robert F., Semenov D., 2014 in Beuther H., Klessen R., Dullemond C., Henning T., eds, Protostars and Planets VI. Univ. Arizona Press, Tucson, AZ, p. 859
Cheng B.-M., Chew E. P., Liu C.-P., Bahou M., Lee Y.-P., Yung Y. L., Gerstell M. F., 1999, Geophys. Res. Lett., 26, 3657
Chick K.M, Cassen P., 1997, ApJ, 477, 398
Clairemidi J., Bréchignac P., Moreels G., Pautet D., 2004, Planet. Space Sci., 52, 761
Cochran A. L., Cochran W. D., 2002, Icarus, 157, 297
Crawford M. K., Tielens A. G. G. M., Allamandola L. J., 1985, ApJ, 293, L45
Davidsson B. J. R. et al., 2016, A&A, 592, A63
Draine B. T., 2003, Annu. Rev. Astron. Astrophys., 41, 241
Drouart A., Dubrulle B., Gautier D., Robert F., 1999, Icarus 140, 129
Dwek E. et al., 1997. ApJ, 475, 565
Elyajouri M., Lallement R., Monreal-Ibero A., Capitanio L., Cox N. L. J., 2017, A&A, 600, A129
Ensor T., Cami J., Bhatt N. H., Soddu A., 2017, ApJ, 836, 162
Foing B., Ehrenfreund P., 1994, Nature, 369, 296
Fomenkova M. N., 1999, Space Sci. Rev., 90, 109
Fray N. et al., 2016, Nature, 538, 72
Friedman S. D. et al., 2011, ApJ, 727, 33
Goesmann F. et al., 2015, Science, 349, aab0689
Greenberg J. M., 1982, in Wilkening L. L. ed, Comets. Univ. Arizona press, Tucson, AZ, p. 131
Greenberg J. M., 1998, A&A, 330, 375
Hamano S. et al., ApJ, 821, 42, 2016
Hartogh P. et al., 2011, Nature, 478, 218
Hässig M. et al., 2015, Science, 347, a0276H
Hobbs L. et al., 2009, ApJ, 705, 32
Jessberger E. K., Kissel J., 1991, in Newburn R. et al. eds, Comets in the Post-Halley Era. Springer-Verlag, Heidelberg, p. 1075
Jessberger E. K., Christoforidis A., Kissel J., 1988, Nature, 332, 691
Joblin C., Leger A., Martin P., 1992, ApJ, 393, L79
Jones A., 2014, Planet. Space Sci., 100, 26
Jones A., 2016, R. Soc. Open Sci., 3, 160223
Kavelaars J. J. et al., 2011, ApJ, 734, L30
Kissel J. et al., 1986, Nature, 321, 280
Krelowski J., Sneden C., 1995, in Tielens A. G. G. M., Snow T. P., eds, Astrophysics and Space Science Library, Vol. 202, The Diffuse Interstellar Bands. Kluwer, Dordrecht, p. 13
Lan T. W., Ménard B., Zhu G., 2015, MNRAS, 452, 3629
Langevin Y., Kissel J., Bertaux J.-L., Chassefiere E., 1987, A&A, 187:761–66
Léger A., D'Hendecourt L., 1985, A&A, 146, 81
Léger A., Puget J. L., 1984, A&A, 137, L5
Linsky J. L. et al., 2006, ApJ. 647, 1106
Lodders K., Palme H., 2009, 72nd Annual Meteoritical Society Meeting, 5154.pdf
McCall B. J. et al., 2010, ApJ, 708, 1628
Mégier A., Aiello S., Barsella B., Casu S., Krełowski J., 2001, MNRAS, 326, 1095
Montillaud J., Joblin C., Toublanc D., 2013, A&A, 552, A15
Moreels G., Clairemidi J., Hermine P., Brechignac P., Rousselot P., 1994, A&A, 282, 643
O'Malia K. K. J., Thorburn J. A., Hammergren M., Snow T. P., Dembicky J., Hobbs L. M., York D. G., 2010, ApJ, 708, 785
Omont A., 2016, A&A, 590, 52
Pering K., Ponnemperuma C., 1971, Science, 173, 237
Rubin M., Altwegg K., van Dishoeck E. F., Schwehm G., 2015, ApJ, 815, L11
Sagdeev R. et al., 1986, Pis'ma Astron Zh., 12, 605
Salama F., Galazutdinov G. A., Krełowski J., Biennier L., Beletsky Y., Song I.-O., 2011, ApJ, 728, 154
Sarre P. J., 2006, J. Mol. Spectrosc., 238, 1
Smith K. T., Fossey S. J., Cordiner M. A., Sarre P. J., Smith A. M., Bell T. A., Viti S., 2013, MNRAS, 429, 939
Snow T. P., 2002, ApJ, 567, 407
Snow T. P., 2014, in Cami J., Cox N. L. J., eds, Proc. IAU Symp. 297, The Diffuse Interstellar Bands. Cambridge Univ. Press, Cambridge, p. 3
Snow T. P., Destree J. D., 2011, in Joblin C., Tielens A., eds, EAS Publ. Ser., edited by EDP Science, Vol. 46, p. 341
Snow T. P., Welty D. E., Thorburn J., Hobbs L. M., McCall B. J., Sonnentrucker P., York D. G., 2002a, ApJ, 573, 670
Snow T. P., Zukowski D., Massey P., 2002b, ApJ, 578, 877
Thi W.-F., Woitke P., Kamp I., 2010, MNRAS, 407, 232
Thorburn J. A. et al., 2003, ApJ, 584, 339
Tielens A. G. G. M., 2013, Rev. Mod. Phys., 85, 1021
Van der Zwet G. P., Allamandola L. J., 1985, A&A, 146, 76
Van Loon J., Smith K. T., McDonald I., Sarre P. J., Fossey S. J., Sharp R. G., 2009, MNRAS, 399, 195
Vos D. A. I., Cox N. L. J., Kaper L., Spaans M., Ehrenfreund P., 2011, A&A, 533, 129
Weinberg D. H., 2016 preprint (arXiv:1604.07434)
Whipple F. L., 1951, ApJ, 113, 464
Xiang F. Y., Li A, Zhong J. X., 2017, ApJ, 835, 107
Yang L., Ciesla F. J., Alexander C. M. O.'D., 2013, Icarus 226, 256
Zasowski G. et al., 2015, ApJ, 798, 35

This paper has been typeset from a Microsoft Word file prepared by the author.